THE JOURNAL OF BIOLOGICAL CHEMISTRY VOL. 290, NO. 15, pp. 9442–9454, April 10, 2015

β-Cyclodextrin-threaded Biocleavable Polyrotaxanes Ameliorate Impaired Autophagic Flux in Niemann-Pick Type C Disease*

Received for publication, January 8, 2015, and in revised form, February 17, 2015 Published, JBC Papers in Press, February 24, 2015, DOI 10.1074/jbc.M115.636803

Atsushi Tamura and Nobuhiko Yui[1]

From the Department of Organic Biomaterials, Institute of Biomaterials and Bioengineering, Tokyo Medical and Dental University, Tokyo 101-0062, Japan

Background: Niemann-Pick type C (NPC) disease is associated with the impaired autophagic flux.
Results: β-Cyclodextrin (β-CD)-threaded polyrotaxanes reduced autophagosome accumulation, promoted autophagic proteolysis, and facilitated the fusion of autophagosomes and lysosomes in NPC disease, whereas β-CD derivatives further disturbed autophagic flux.
Conclusion: β-CD-threaded polyrotaxanes improved impaired autophagic flux in NPC disease.
Significance: β-CD-threaded polyrotaxanes may be promising therapeutics for ameliorating impaired autophagy in NPC disease.

Niemann-Pick type C (NPC) disease is characterized by the lysosomal accumulation of cholesterols and impaired autophagic flux due to the inhibited fusion of autophagosomes to lysosomes. We have recently developed β-cyclodextrin (β-CD)-threaded biocleavable polyrotaxanes (PRXs), which can release threaded β-CDs in response to intracellular environments as a therapeutic for NPC disease. The biocleavable PRXs exhibited effective cholesterol reduction ability and negligible toxic effect compared with hydroxypropyl-β-CD (HP-β-CD). In this study, we investigated the effect of biocleavable PRX and HP-β-CD on the impaired autophagy in NPC disease. The NPC patient-derived fibroblasts (NPC1 fibroblasts) showed an increase in the number of LC3-positive puncta compared with normal fibroblasts, even in the basal conditions; the HP-β-CD treatment markedly increased the number of LC3-positive puncta and the levels of p62 in NPC1 fibroblasts, indicating that autophagic flux was further perturbed. In sharp contrast, the biocleavable PRX reduced the number of LC3-positive puncta and the levels of p62 in NPC1 fibroblasts through an mTOR-independent mechanism. The mRFP-GFP-LC3 reporter gene expression experiments revealed that the biocleavable PRX facilitated the formation of autolysosomes to allow for autophagic protein degradation. Therefore, the β-CD-threaded biocleavable PRXs may be promising therapeutics for ameliorating not only cholesterol accumulation but also autophagy impairment in NPC disease.

Niemann-Pick type C (NPC)[2] disease is an autosomal recessive lysosomal storage disorder caused by the mutation of NPC1 (1–3). Because NPC1 is a key transmembrane protein for transferring low density lipoprotein-derived cholesterols from endosomes/lysosomes to the endoplasmic reticulum, a dysfunction in NPC1 proteins cause lysosomal accumulation of unesterified cholesterols. Due to the lysosomal accumulation of cholesterols, patients with NPC disease exhibit various clinical symptoms, including neurodegeneration and hepatosplenomegaly (4, 5). Hydroxypropyl-β-cyclodextrin (HP-β-CD), a cyclic oligosaccharide derivative, has recently attracted considerable attention as a therapeutic for NPC disease (6–9). The administration of HP-β-CD has been reported to remarkably prolong the life span of *Npc1*$^{-/-}$ mice through a reduction in cholesterol levels (6–8). To further develop a β-CD-based therapy for NPC disease, we have developed β-CD-threaded biocleavable polyrotaxanes (PRXs), a class of polymeric supermolecules composed of cyclic compounds threaded onto a linear polymer chain (10, 11), for the lysosome-specific delivery of β-CDs (Fig. 1) (12). The β-CD-threaded PRXs bearing cleavable disulfide linkages showed less interaction with the plasma membrane than did HP-β-CD, leading to internalization into late endosomes/lysosomes through endocytosis (Fig. 1) (12). Due to this preferential transportation to lysosomes as well as to the local release of threaded β-CDs by the cleavage of terminal disulfide linkages in the intracellular reductive environment, the biocleavable PRXs effectively reduced lysosomal cholesterols to a 100-fold lower concentration than did HP-β-CD

* This work was supported by Grant-in-aid for Scientific Research 23107004 on Innovative Areas "Nanomedicine Molecular Science" (to N. Y.) from the Ministry of Education, Culture, Sports, Science, and Technology (MEXT) of Japan; Grant-in-Aid for Young Scientists (B) 26750155 (to A. T.) from MEXT of Japan; and the Mochida Memorial Foundation for Medical and Pharmaceutical Research (to A. T.).
[1] To whom correspondence should be addressed: Dept. of Organic Biomaterials, Institute of Biomaterials and Bioengineering, Tokyo Medical and Dental University, 2-3-10 Kanda-Surugadai, Chiyoda, Tokyo 101-0062, Japan. Tel.: 81-3-5280-8020; Fax: 81-3-5280-8027; E-mail: yui.org@tmd.ac.jp.

[2] The abbreviations used are: NPC, Niemann-Pick type C; CD, cyclodextrin; PRX, polyrotaxane; HEE-SS-PRX, (2-hydroxyethoxy)ethyl group-modified biocleavable polyrotaxane bearing terminal disulfide linkages; HP-β-CD, hydroxypropyl-β-cyclodextrin; LC3, microtubule-associated protein 1 light chain 3; mTORC1, mammalian target of rapamycin complex 1; LAMP1, lysosome-associated membrane protein 1; M_n, number average molecular weight; mRFP, monomeric RFP; DM-β-CD, heptakis(2,6-di-*O*-methyl)-β-cyclodextrin; Baf A, bafilomycin A1; HEE, (2-Hydroxyethoxy)ethyl; CDI, *N*,*N*′-carbonyldiimidazole; HEEA, 2-(2-hydroxyethoxy)ethylamine; Z, benzyloxycarbonyl; CLSM, confocal laser scanning microscopy; GM1, monosialotetrahexosylganglioside.

(12). Additionally, the biocleavable PRXs were shown to induce a negligible extraction of cholesterols from the plasma membrane, whereas HP-β-CD extracted high levels of cholesterols from the plasma membrane, indicating that the site of cholesterol reduction is different between the biocleavable PRXs and HP-β-CD (12). Therefore, the biocleavable PRXs are considered to act as an intracellular delivery vehicle for β-CDs or as a type of prodrug for enhancing their therapeutic effect.

Moreover, autophagy, a bulk degradation system of cytoplasmic protein aggregates and subcellular organelles, is of increasing importance with respect to its relation to various diseases. Basal autophagy plays a pivotal role in the constitutive turnover of cytoplasmic components for maintaining cellular function (13–16). It is known that $Atg5^{-/-}$ or $Atg7^{-/-}$ mice display neurodegeneration and hepatomegaly, indicating that basal autophagy is strongly related to a variety of pathological states (17, 18). Indeed, impaired basal autophagy has been reported in various neurodegenerative diseases and lysosomal storage disorders (19, 20), including Niemann-Pick type A disease (21), Fabry disease (22), GM1 gangliosidosis (23), multiple sulfatase deficiency (24), Dannon disease (25), Batten disease (26), and NPC disease (27–33). It has been suggested that the major pathological states of lysosomal storage disorders are attributed to impaired basal autophagy (15, 20). In most of these diseases, abundant autophagosomes accumulate in the cytoplasmic compartments under basal conditions (19, 20). In NPC disease, various researchers have reported autophagosome accumulation even in the basal condition (27–33). To date, various possibilities have been suggested for the mechanism of impaired autophagy in NPC disease, such as a decline in the lysosomal enzymatic activity due to lysosomal cholesterol accumulation (32) and an impaired fusion of autophagosomes with lysosomes (33). Therefore, an improvement in impaired autophagy is required for the treatment of NPC disease in addition to a chronic cholesterol accumulation in lysosomes. Jaenisch and co-workers (33) have reported that HP-β-CD induces the decline of autophagic flux in normal and NPC1 model cells. This indicates that the simultaneous improvement of cholesterol accumulation and impaired autophagy in NPC disease is still a challenging issue.

In this study, we investigated the effect of biocleavable PRXs on autophagy impairment in NPC patient-derived fibroblasts in comparison with HP-β-CD. We found that the biocleavable PRXs could remarkably improve the impaired autophagic flux by facilitating the formation of autolysosomes, although HP-β-CD induced autophagosome accumulation. Notably, the biocleavable PRXs exhibited an effect opposite to that of HP-β-CD on impaired autophagy in NPC disease, although both were able to reduce lysosomal cholesterol levels.

EXPERIMENTAL PROCEDURES

Materials—HP-β-CD (332607, M_n = 1,460) and heptakis(2,6-di-*O*-methyl)-β-cyclodextrin (DM-β-CD) were obtained from Sigma-Aldrich. Bafilomycin A1 (Baf A) was obtained from Wako Pure Chemicals (Osaka, Japan).

Synthesis of (2-Hydroxyethoxy)ethyl (HEE) Group-modified Biocleavable Pluronic P123/β-CD Polyrotaxanes—Pluronic P123/β-CD-based PRX bearing reduction-cleavable disulfide linkages capped with *N*-(triphenylmethyl)glycine was synthesized as described previously (12). The P123/β-CD PRXs with a number of threading β-CDs of 16.1 were used in this study. To a solution of the PRX (250 mg, 9.8 μmol) in anhydrous DMSO (15 ml), *N*,*N*′-carbonyldiimidazole (CDI) (Sigma-Aldrich) (203 mg, 1.26 mmol) was added at room temperature. After a 24-h reaction, 2-(2-hydroxyethoxy)ethylamine (HEEA) (TCI, Tokyo, Japan) (624 μl, 6.29 mmol) was added to the reaction mixture and stirred for a further 24 h at room temperature. Then the PRX was purified by dialysis against methanol for 3 days (Spectra/Por 6, molecular weight cut-off of 3,500). The recovered solution was evaporated and dissolved in water. The aqueous solution was freeze-dried to obtain P123/β-CD HEE-SS-PRX (237.6 mg, 71.4% yield). The number of modified HEE groups on PRX was determined by the ^{1}H NMR (Bruker Avance III 500-MHz spectrometer, Bruker BioSpin, Rheinstetten, Germany). The numbers of threading β-CDs and HEE groups on PRX were determined to be 16.1 and 64.7, respectively. The $M_{n,\mathrm{NMR}}$ of HEE-SS-PRX was determined to be 34,100.

Synthesis of HEE Group-modified β-CD (HEE-β-CD)—To a solution of β-CD (1.0 g, 881 μmol) in dehydrated DMSO (15 ml), CDI (1.72 g, 10.6 mmol) was added at room temperature. After the reaction for 24 h, HEEA (5.25 ml, 52.9 mmol) was added to the reaction mixture and stirred for a further 24 h at room temperature. Then the PRX was purified by dialysis against methanol for 4 days (Spectra/Por 6; molecular weight cut-off of 1,000). The recovered solution was evaporated and dissolved in water. The aqueous solution was freeze-dried to obtain HEE-β-CD (186.9 mg, 12.4% yield). The number of modified HEE groups on β-CD was determined to be 4.3 by the ^{1}H NMR. The $M_{n,\mathrm{NMR}}$ of HEE-β-CD was determined to be 1,700.

Synthesis of HEE Group-modified Biocleavable PEG/α-CD Polyrotaxanes—The PEG/α-CD-based PRX bearing reduction-cleavable disulfide linkages capped with *N*-benzyloxycarbonyl-L-tyrosine (Z-Tyr-OH) was synthesized as described previously (34). The PEG/α-CD-based PRXs with a number of threading α-CDs of 30.7 and an M_n of PEG axle of 9,810 were used in this study. To a solution of the PRX (200 mg, 4.9 μmol) in anhydrous DMSO (5 ml), CDI (196 mg, 1.21 mmol) was added at room temperature. After the reaction for 24 h, HEEA (1.2 ml, 12.1 mmol) was added to the reaction mixture and stirred for a further 24 h at room temperature. The PRX was purified as described above to obtain PEG/α-CD HEE-SS-PRX (212.5 mg, 79.6% yield). The numbers of threading α-CDs and HEE groups on PRX were determined to be 30.7 and 104.5, respectively. The $M_{n,\mathrm{NMR}}$ of HEE-SS-PRX was determined to be 54,200.

Synthesis of HEE Group-modified P123/α-CD Biocleavable Polyrotaxanes—P123 bearing terminal cystamine (P123-SS-NH_2) was synthesized as previously described (12). P123-SS-NH_2 (1.0 g, 147 μmol) dissolved in a small aliquot of water was added to the saturated solution of α-CD (Ensuiko Sugar Refining, Tokyo, Japan) (4.0 g, 4.11 mmol) (27.6 ml), and the system was stirred for 24 h at room temperature. After the reaction, the precipitate was collected by centrifugation (7,000 rpm, 10 min) and freeze-dried for 1 day to obtain pseudopolyrotaxane (2.88 g). Then, to a solution of Z-Tyr-OH (Sigma-Aldrich) (1.85 g,

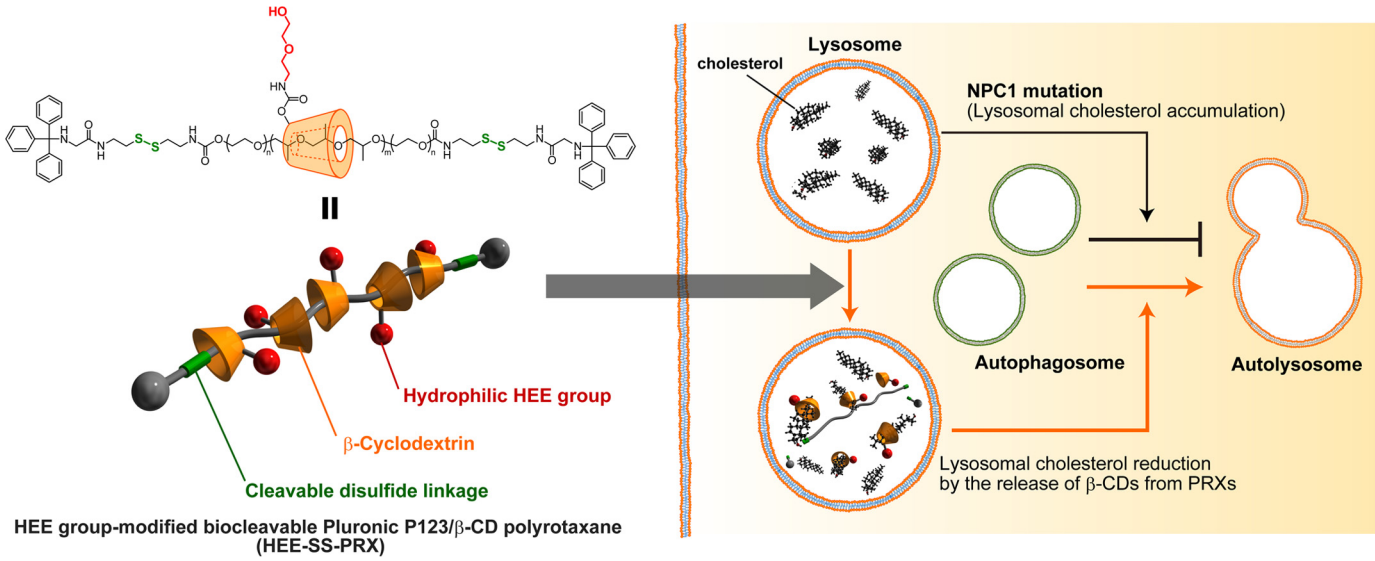

FIGURE 1. **Schematic illustration of β-CD-threaded biocleavable PRXs and the impaired autophagic flux in NPC disease.** The NPC1 mutation hinders the fusion of autophagosomes to lysosomes, whereas treatment with the biocleavable PRXs facilitates autolysosome formation.

5.88 mmol) and 4-(4,6-dimethoxy-1,3,5-triazin-2-yl)-4-methylmorpholinium chloride (Wako) (1.63 g, 5.88 mmol) in methanol (23 ml), the pseudopolyrotaxane was added. The resulting reaction mixture was stirred for 24 h at room temperature. After the reaction, the precipitate was successively washed with *N*,*N*-dimethylformamide and water. The recovered PRX was freeze-dried to obtain P123/α-CD PRX (226.8 mg, 7.8% yield based on P123 mol%). The number of α-CDs threaded onto the PRX was 13.1, as determined by ^{1}H NMR. Then, to a solution of the PRX (200 mg, 10.0 μmol) in anhydrous DMSO (10 ml), CDI (176 mg, 1.08 mmol) was added at room temperature. After the reaction for 24 h, HEEA (1.07 ml, 10.8 mmol) was added to the reaction mixture and stirred for a further 24 h at room temperature. The PRX was purified as described above to obtain P123/α-CD HEE-SS-PRX (216.8 mg, 76.4% yield). The numbers of threading α-CDs and HEE groups on PRX were determined to be 13.1 and 57.5, respectively. The $M_{n,\mathrm{NMR}}$ of HEE-SS-PRX was determined to be 28,300.

Cell Culture—Human dermal fibroblasts derived from a Niemann-Pick type C disease patient (NPC1) (GM03123; P237S and I1061T mutations in NPC1) and normal human dermal fibroblasts (GM05659) were obtained from the Coriell Institute for Medical Research (Camden, NJ). These cells were grown in Dulbecco's modified Eagle's medium (DMEM) (Gibco) containing 10% fetal bovine serum (FBS) (Gibco), 100 units/ml penicillin (Gibco), and 100 μg/ml streptomycin (Gibco) in a humidified 5% CO_2 atmosphere at 37 °C. For treatment with HP-β-CD, HEE-SS-PRX, and Baf A, the normal and NPC1 fibroblasts were seeded into a 12-well plate (Nunc, Roskilde, Denmark) at a density of 1×10^5 cells/well and incubated overnight. After the medium was exchanged with fresh medium (900 μl), the treatment solutions (100 μl) were applied to each well, followed by incubation for 24 h at 37 °C. To induce autophagy via amino acid starvation, the cells were cultured in Hanks' balanced salt solution (Sigma-Aldrich) at 37 °C. For microscopic observation of the treated cells, the cells were seeded into a 35-mm glass-bottomed dishes (Iwaki Glass, Tokyo, Japan) at a density of 1×10^4 cells/dish and incubated overnight. After the medium was exchanged with fresh DMEM (270 μl), the treatment solutions (30 μl) were applied to the dish, followed by incubation for 24 h at 37 °C.

Immunocytochemical and Filipin Staining—After treatment, the cells were washed twice with PBS, fixed with 4% paraformaldehyde for 15 min at room temperature, permeabilized with 50 μg/ml digitonin (Wako) for 5 min at room temperature, and blocked with 1% bovine serum albumin (BSA) (Sigma-Aldrich) for 1 h at room temperature. The cells were then treated with the following primary antibodies for 1 h at room temperature: rabbit polyclonal anti-LC3 (PM036, MBL (Nagoya, Japan); 1:100 dilution) and mouse monoclonal anti-lysosome-associated membrane protein 1 (LAMP1) (sc-20011, Santa Cruz Biotechnology, Inc.; 1:200 dilution). Finally, the cells were stained with the following secondary antibodies for 30 min at room temperature: Alexa Fluor 488-conjugated goat anti-rabbit IgG (Molecular Probes, Inc., Eugene, OR) and Alexa Fluor 488-conjugated goat anti-mouse IgG (Abcam, Cambridge, MA). For staining unesterified cholesterols, the cells were stained with filipin (PolySciences, Warrington, PA) (50 μg/ml) for 45 min. Confocal laser scanning microscopy (CLSM) images were acquired with a FluoView FV10i microscope (Olympus, Tokyo, Japan) equipped with a ×60 water immersion objective lens (numerical aperture 1.2) and a diode laser.

Quantification of Total Cholesterol—After treatment, the cells were washed three times with PBS. The cells were then harvested with trypsin-EDTA, washed several times with PBS, and lysed with cell lysis buffer (100 mM phosphate buffer, 1 M NaCl, 50 mM cholic acid, and 1% Triton X-100). The total cholesterol (the sum of esterified and unesterified cholesterols) was determined using an Amplex Red cholesterol assay kit (Molecular Probes). Briefly, sample solution (50 μl) was combined with the assay solution (50 μl) containing cholesterol esterase (2 units/ml), cholesterol oxidase (2 units/ml), horseradish peroxidase (2 units/ml), and Amplex Red reagent (fluorescent sub-

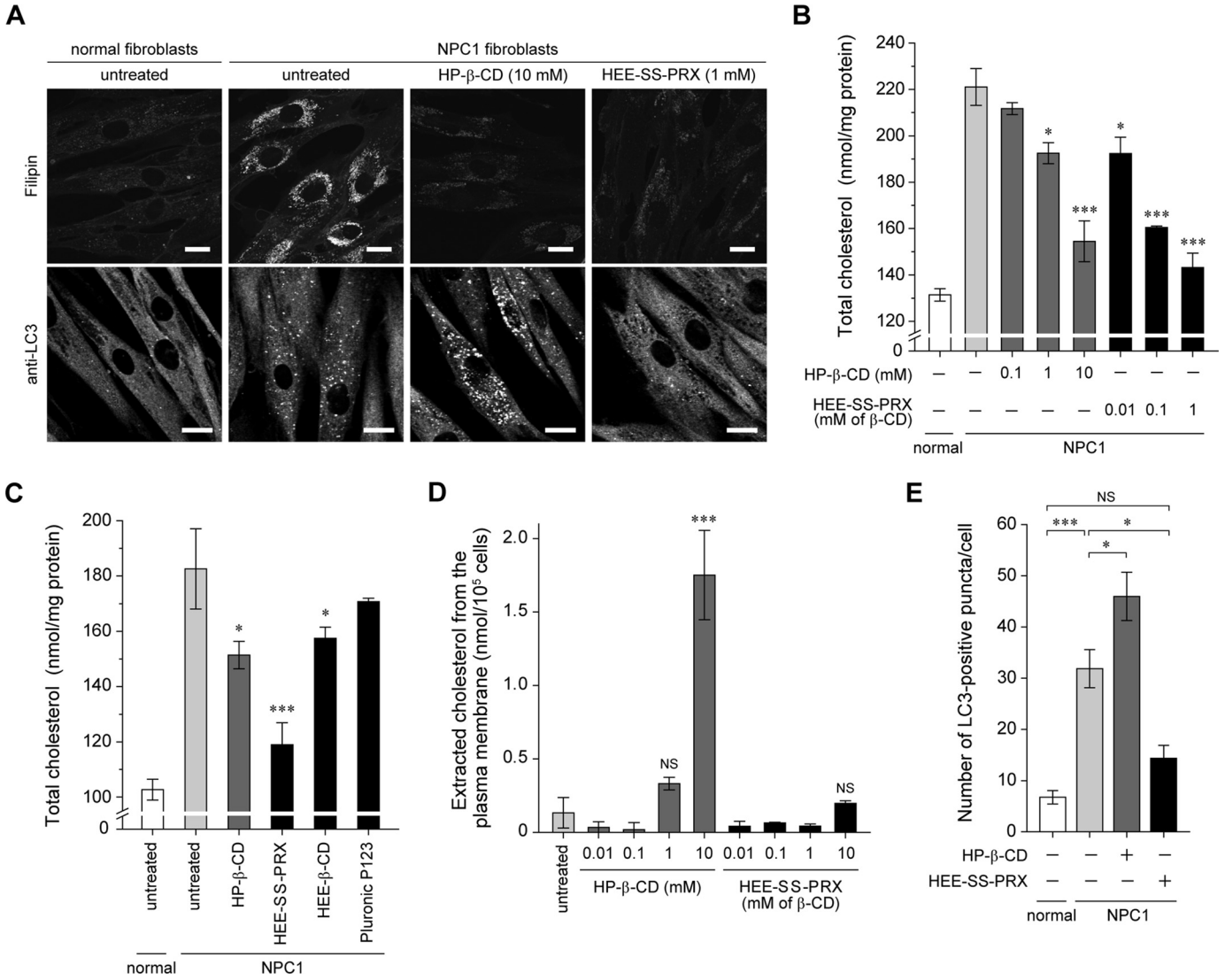

FIGURE 2. **The effect of HP-β-CD and a biocleavable polyrotaxanes on the lysosomal cholesterol accumulation and impaired autophagy in NPC1 fibroblasts.** *A*, filipin staining for cholesterol and anti-LC3 staining for autophagosomes in the normal and NPC1 fibroblasts treated with HP-β-CD (10 mM) and HEE-SS-PRX (1 mM β-CD) for 24 h (*scale bars*, 20 μm). *B*, the amount of total cholesterol in the normal and NPC1 fibroblasts treated with HP-β-CD and HEE-SS-PRX at various concentrations for 24 h ($n = 3$) (*, $p < 0.05$; **, $p < 0.01$; ***, $p < 0.005$ against untreated NPC1 fibroblasts). *Error bars*, S.D. *C*, the amount of total cholesterol in the normal and NPC1 fibroblasts treated with HP-β-CD (1 mM), HEE-SS-PRX (1 mM β-CD and 58 μM Pluronic P123), HEE-β-CD (1 mM), and Pluronic P123 (58 μM) for 24 h ($n = 3$) (*, $p < 0.05$; ***, $p < 0.005$ against untreated NPC1 fibroblasts). *Error bars*, S.D. *D*, the amount of extracted cholesterol from the plasma membrane of the NPC1 fibroblasts treated with HP-β-CD and HEE-SS-PRX at various concentrations for 2 h at 4 °C ($n = 3$) (***, $p < 0.005$ against untreated NPC1 fibroblasts; *NS*, not significant). *Error bars*, S.D. *E*, the number of LC3-positive puncta in the normal and NPC1 fibroblasts treated with HP-β-CD (10 mM) and HEE-SS-PRX (1 mM β-CD) for 24 h. The values are expressed as the mean ± S.E. (*error bars*) of 30 cells (*, $p < 0.05$; ***, $p < 0.005$; *NS*, not significant).

strate) (300 μM) and incubated for 30 min at 37 °C. The fluorescence intensities were measured on an ARVO MX multilabel counter (PerkinElmer Life Sciences) equipped with a filter set for excitation and emission at 560 ± 10 nm and 590 ± 10 nm, respectively. Protein content in the lysate was also determined with a Micro BCA protein assay kit (Thermo Fisher Scientific). Cellular cholesterol content was normalized to protein content and expressed as nmol/mg of protein.

Cholesterol Extraction from the Plasma Membrane—After the treatment of NPC1 fibroblasts in Hanks' balanced salt solution for 2 h at 4 °C, the supernatant was collected. The concentration of cholesterol in the supernatant was determined by the Amplex Red cholesterol assay kit as described above.

Immunoblotting—After treatment, the cells were washed three times with PBS and lysed with radioimmune precipitation buffer (50 mM Tris-HCl, 150 mM NaCl, 0.5% sodium deoxycholate, 0.1% SDS, 1% Nonidet P-40 substitute, pH 8.0) containing protease inhibitors (Nacalai Tesque, Tokyo, Japan) and phosphatase inhibitors (Nacalai Tesque). The lysates were clarified by centrifugation at 15,000 rpm for 10 min, and the supernatant was collected. The supernatant was mixed with the sample buffer and incubated at 98 °C for 1 min. SDS-PAGE was performed on a 12% gel for 50 min at 150 V (in the case of 4E-BP1 immunoblotting, the electrophoresis was performed on a 18% gel for 180 min at 150 V). The samples were then transferred to a PVDF membrane (Bio-Rad) using a Trans-Blot Turbo transfer system (Bio-Rad). The membrane was blocked with TBST (20 mM Tris-HCl, 500 mM NaCl, 0.05% Tween 20, pH 7.5) containing 5% BSA for 60 min at room temperature. Then the membrane was treated overnight with the following

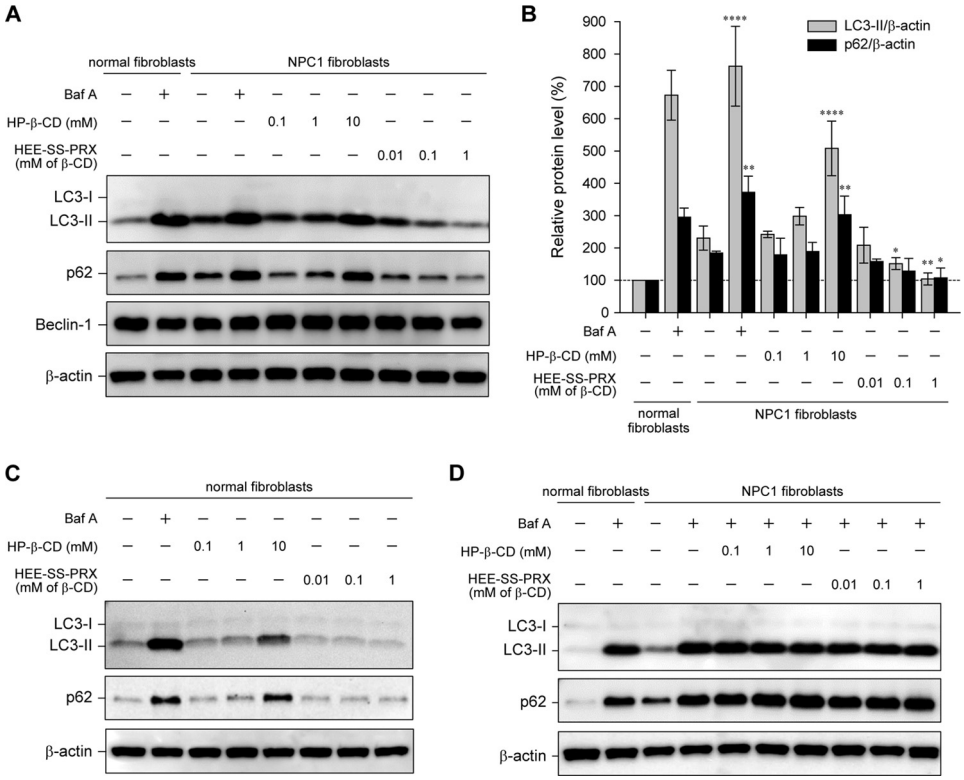

FIGURE 3. **HP-β-CD and biocleavable polyrotaxanes had opposite effects on the levels of LC3-II and p62.** *A*, immunoblot analysis for LC3, p62, Beclin-1, and β-actin in the normal and NPC1 fibroblasts treated with Baf A (400 nM), HP-β-CD, and HEE-SS-PRX at various concentrations for 24 h. *B*, relative protein level for LC3-II/β-actin (*gray bars*) and p62/β-actin (*black bars*) as determined by the band intensities of the immunoblot. The intensity of each band was normalized with β-actin (*, $p < 0.05$; **, $p < 0.01$; ****, $p < 0.001$). *C*, immunoblot analysis for LC3, p62, and β-actin in the normal fibroblasts treated with Baf A (400 nM), HP-β-CD, and HEE-SS-PRX at various concentrations for 24 h. *D*, immunoblot analysis for LC3, p62, and β-actin in the NPC1 fibroblasts treated with HP-β-CD and HEE-SS-PRX in the presence of Baf A (400 nM) for 24 h. The values are expressed as the mean ± S.D. (*error bars*) ($n = 3$).

primary antibodies at 4 °C: rabbit polyclonal anti-LC3 (PM036, MBL; 1:1,000 dilution), rabbit polyclonal anti-p62/SQSTM1 (PM045, MBL; 1:2,000 dilution), rabbit monoclonal anti-Beclin-1 (3495, Cell Signaling Technologies (Danvers, MA); 1:1000 dilution), rabbit monoclonal anti-p70 S6K (2708, Cell Signaling Technologies; 1:500 dilution), rabbit monoclonal anti-phospho-p70 S6K (9234, Cell Signaling Technologies; 1:500 dilution), rabbit monoclonal anti-4E-BP1 (9452, Cell Signaling Technologies; 1:1,000 dilution), rabbit polyclonal anti-cathepsin B (ab33538, Abcam; 1:300 dilution), and rabbit polyclonal anti-β-actin (A2066, Sigma-Aldrich; 1:2,000 dilution). The membrane was treated with horseradish peroxidase (HRP)-conjugated goat anti-rabbit IgG (MBL) for 60 min at room temperature. Finally, the membrane was visualized with the ECL Prime or ECL Select Western blotting detection system (GE Healthcare). The chemiluminescence images were acquired on an ImageQuant LAS 500 imager (GE Healthcare), and the intensity of the bands was analyzed using ImageJ software version 1.45s (National Institutes of Health, Bethesda, MD).

Plasmid DNAs and Transfection—Plasmid DNAs encoding mRFP-GFP tandem fluorescence-tagged LC3 (pmRFP-GFP-LC3) (catalog no. 21074) and mRFP-LC3 (catalog no. 21075) were obtained from Addgene (Cambridge, MA) (35). The normal and NPC1 fibroblasts were plated into 35-mm glass-bottomed dishes at a density of 1×10^4 cells/dish and treated with transfection solutions containing 250 ng of plasmid DNA and Lipofectamine 3000 (Life Technologies, Inc.). After 24 h of incubation, the cells were washed three times with culture medium. The treatment solutions (30 μl) were then applied to the dishes, followed by incubation for 24 h. The CLSM images were acquired with a FluoView FV10i imager.

Cathepsin B Activity—After treatment, the cells were washed twice with PBS and fixed with 4% paraformaldehyde for 15 min at room temperature. The cells were then stained with the Magic Red cathepsin B detection kit (Immunochemistry Technologies, Bloomington, MN) according to the manufacturer's instructions. The CLSM images were acquired with a FluoView FV10i imager. For the fluorescence intensity measurements, the cells were harvested and stained with Magic Red cathepsin B. After incubation for 1 h at 37 °C, the fluorescence intensities were measured on an ARVO MX multilabel counter.

Statistical Analysis—The data are presented as the mean ± S.D. Differences between the means of the individual groups were assessed by one-way analysis of variance followed by Tukey's multiple comparison test. A p value of less than 0.05 was considered as statistically significant.

RESULTS

Design of Biocleavable Polyrotaxanes and Their Effect on Lysosomal Cholesterol and Autophagosomes Accumulation in NPC1 Fibroblasts—The biocleavable PRXs composed of Pluronic P123 and β-CD capped with (*N*-triphenylmethyl)glycine via intracellular cleavable disulfide linkages were synthesized (Fig. 1). HEE groups were chemically modified on the hydroxyl

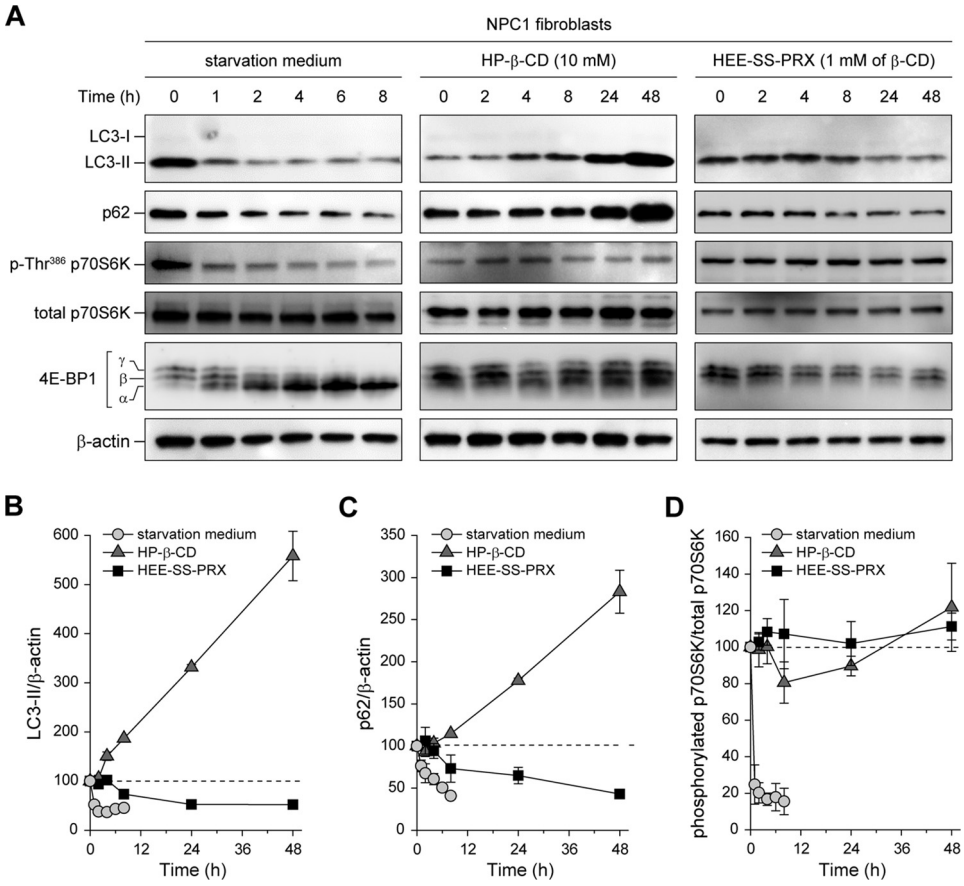

FIGURE 4. **The activity of mTORC1 in the NPC1 fibroblasts treated with HP-β-CD and biocleavable polyrotaxanes.** *A*, time courses of the expression levels for LC3, p62, phospho-Thr^{386} S6K, total S6K, 4E-BP1, and β-actin in the NPC1 fibroblasts after treatment with starvation medium, HP-β-CD (10 mM), and HEE-SS-PRX (1 mM β-CD). *B–D*, time course of relative band intensity changes for LC3-II/β-actin (*B*), p62/β-actin (*C*), and phospho-Thr^{386} S6K/total S6K (*D*) in NPC1 fibroblasts treated with starvation medium (*circles*), HP-β-CD (10 mM) (*triangles*), and HEE-SS-PRX (1 mM β-CD) (*squares*) ($n = 3$). The values are expressed as the mean ± S.D. (*error bars*).

groups of β-CD in PRX to impart water solubility (denoted as HEE-SS-PRX). To confirm the cholesterol reduction ability of HEE-SS-PRX in NPC disease patient-derived fibroblasts (NPC1 fibroblasts), filipin staining for cholesterol and the quantification of total cholesterol (the sum of esterified and unesterified cholesterols) were performed in comparison with HP-β-CD (Fig. 2, *A* and *B*). The lysosomal cholesterol in NPC1 fibroblasts was reduced to levels almost comparable with the normal levels by both HP-β-CD (10 mM) and HEE-SS-PRX (1 mM β-CD) treatments, indicating that lysosomal release of threaded β-CDs from HEE-SS-PRX may be attributable to significant cholesterol reduction. To confirm this hypothesis, the cholesterol reduction ability of HEE-SS-PRX was evaluated in comparison with its constituent molecules, such as HEE group-modified β-CD (HEE-β-CD) and the axle polymer (Pluronic P123) (Fig. 3*C*). As a result, HEE-β-CD and P123 exhibited lower ability in cholesterol reduction than HEE-SS-PRX. Accompanied with the lysosomal cholesterol reduction in NPC1 fibroblasts, HP-β-CD concomitantly extracted cholesterols from the plasma membrane, whereas negligible cholesterol extraction from the plasma membrane was observed for the HEE-SS-PRX-treated NPC1 fibroblasts (Fig. 2*D*). Altogether with these results, it is obvious that HEE-SS-PRX reduced lysosomal cholesterol to a much lower concentration than HP-β-CD without cholesterol extraction from the plasma membrane (12). In the present experimental conditions, the number of cells and the concentration of total protein were not decreased by the treatment with HP-β-CD (10 mM) and HEE-SS-PRX (1 mM β-CD), suggesting the negligible toxicity of these treatments.

The accumulation of autophagosomes in NPC1 fibroblasts was evaluated by immunostaining of microtubule-associated protein 1 light chain 3 (LC3), which is a soluble cytosolic protein (LC3-I form), whereas C-terminal modification with phosphatidylethanolamine (LC3-II form) leads to localization at the autophagosomal membrane (36, 37). The number of cytoplasmic LC3-positive puncta in the NPC1 fibroblasts was significantly higher than in the normal fibroblasts just cultured in the growth medium, confirming that the basal autophagy was perturbed by either the mutation of NPC1 or the lysosomal cholesterol accumulation (Fig. 2, *A* and *E*) (27–33). Upon treatment with HP-β-CD, the number of LC3-positive puncta in the NPC1 fibroblasts increased further. By contrast, the number of LC3-positive puncta in NPC1 fibroblasts was decreased to the normal level by treatment with HEE-SS-PRX. Although both HP-β-CD and HEE-SS-PRX were effective in reducing lysosomal cholesterol in NPC1 fibroblasts, their effects on autophagy were opposite.

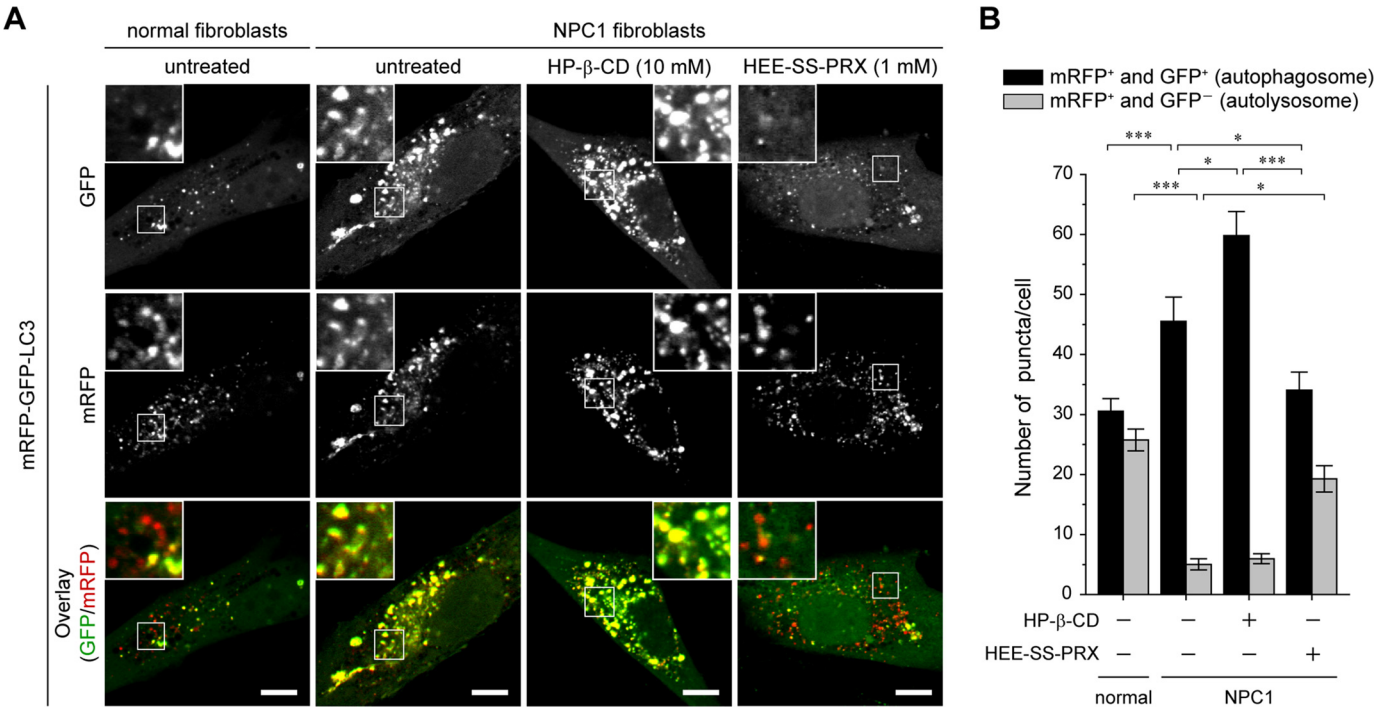

FIGURE 5. **Biocleavable polyrotaxanes improved impaired autophagic flux in NPC1 fibroblasts.** *A*, CLSM images of normal and NPC1 fibroblasts transiently expressing mRFP-GFP-LC3 (*green* and *red puncta* indicate GFP and mRFP, respectively) treated with HP-β-CD (10 mM) and HEE-SS-PRX (1 mM β-CD) for 24 h (*scale bars*, 20 μm). *B*, the numbers of $mRFP^+$-GFP^+ and $mRFP^+$-GFP^- puncta in the normal and NPC1 fibroblasts expressing mRFP-GFP-LC3. The values are expressed as the mean ± S.E. (*error bars*) of 30 cells (*, $p < 0.05$; **, $p < 0.01$; ***, $p < 0.005$).

Improvement of Autophagosomes and p62 Accumulation in NPC1 Fibroblasts by Biocleavable Polyrotaxanes—Further confirmation of these results was obtained by immunoblotting for LC3-II and p62/SQSTM1 (p62), a selective substrate for autophagic protein degradation (Fig. 3, *A* and *B*) (38). Note that the levels of both LC3-II and p62 increased in NPC1 fibroblasts compared with normal fibroblasts even in the basal condition, indicating that the autophagic flux in NPC1 fibroblasts was decreased compared with the normal fibroblasts. Treatment with Baf A, a specific inhibitor of the vacuolar-type H^+-ATPase, resulted in increased levels of both LC3-II and p62 in the normal and NPC1 fibroblasts due to the decrease in lysosomal enzymatic activity by the neutralization of the lysosomal pH (39). Similar to the Baf A treatment, HP-β-CD induced increases in the levels of both LC3-II and p62 in a concentration-dependent manner. By contrast, HEE-SS-PRX reduced the levels of LC3-II and p62 in a concentration-dependent manner, and these protein levels reached levels comparable with those observed in normal fibroblasts at the HEE-SS-PRX concentration equivalent to 1 mM β-CD. HP-β-CD treatments also increased the levels of both LC3-II and p62 in the normal fibroblasts, whereas HEE-SS-PRX treatment showed negligible effects or induced a slight reduction of LC3-II and p62 in the normal fibroblasts (Fig. 3*C*). In the NPC1 fibroblasts treated with HP-β-CD or HEE-SS-PRX in the presence of Baf A, the levels of LC3-II and p62 increased to comparable levels, regardless of the concentrations of HP-β-CD or HEE-SS-PRX (Fig. 3*D*).

mTORC1 Activity in NPC Fibroblasts Treated with HP-β-CD and Biocleavable Polyrotaxanes—The mammalian target of rapamycin complex 1 (mTORC1) plays a pivotal role in the regulation of autophagy (40–42), and the inhibition of mTORC1 activity, such as by amino acid starvation, causes the induction of autophagy. To investigate whether HP-β-CD and HEE-SS-PRX treatments induced mTORC1-dependent autophagy, the dephosphorylation of p70 S6 kinase (p70S6K) and eukaryotic initiation factor 4E-binding protein 1 (4E-BP1) was monitored at various time points during the treatments (Fig. 4*A*). When the NPC1 fibroblasts were cultured in starvation medium, the levels of LC3-II and p62 decreased with time (Fig. 4, *B* and *C*). In addition, the dephosphorylation of Thr-368 of p70S6K and the conversion of the phosphorylated γ-form to the dephosphorylated α-form were observed for 4E-BP1 (Fig. 4*D*) (43). HP-β-CD proportionally increased LC3-II and p62 levels during the treatment time periods, whereas negligible dephosphorylation of p70S6K and 4E-BP1 was observed (Fig. 4, *A*–*D*). HEE-SS-PRX treatment decreased the levels of LC3-II and p62 in the NPC1 fibroblasts, which reached constant levels after 24 h of incubation, but negligible dephosphorylation of p70S6K and 4E-BP1 was observed (Fig. 4, *A*–*D*).

The Maturation of Autophagosomes and the Lysosomal Enzymatic Activity in NPC Fibroblasts—To verify whether the HP-β-CD and HEE-SS-PRX treatments affected the autolysosome formation, autophagic flux in the NPC1 fibroblasts was monitored using an expression vector encoding mRFP-GFP tandem fluorescence-tagged LC3 (mRFP-GFP-LC3) (Fig. 5, *A* and *B*) (35). When the mRFP-GFP-LC3 is localized to the autophagosomes, it emits both mRFP (*red*) and GFP (*green*) signals and appears as *yellow*. By contrast, when the mRFP-GFP-LC3 is localized to the acidic autolysosome, it emits only an mRFP signal and appears as red because the GFP signal quenches immediately under acidic conditions (pK_a of GFP,

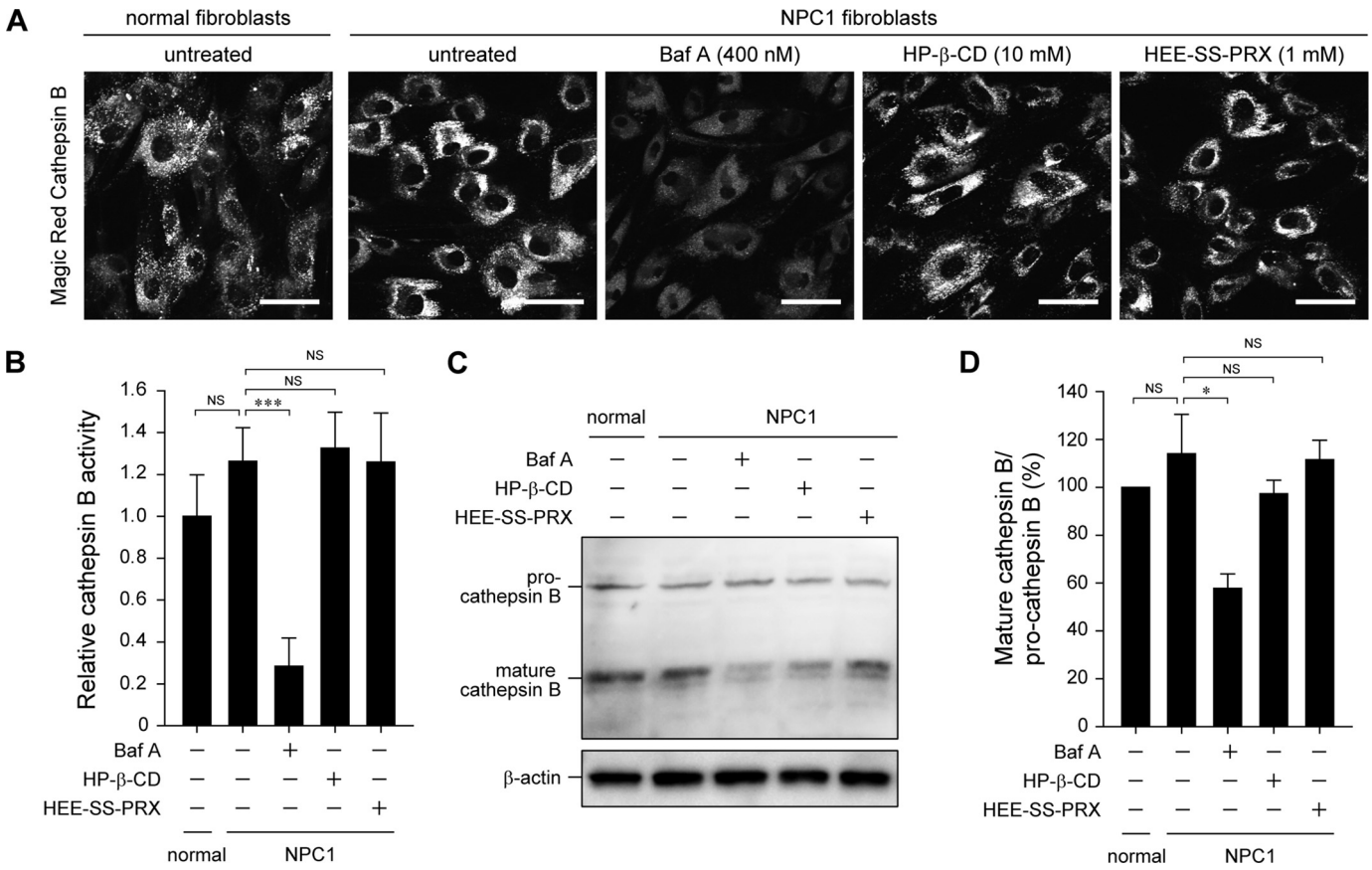

FIGURE 6. **Biocleavable polyrotaxanes do not affect lysosomal enzymatic activity.** *A*, CLSM images of the activity of cathepsin B in the normal and NPC1 fibroblasts treated with Baf A (400 nM), HP-β-CD (10 mM), and HEE-SS-PRX (1 mM) for 24 h, as determined by Magic Red cathepsin B (*scale bars*, 50 μm). *B*, relative fluorescence intensities of the Magic Red cathepsin B. The values are normalized with the untreated normal fibroblasts ($n = 3$) (***, $p < 0.005$; *NS*, not significant). *C*, immunoblot analysis for pro- and mature cathepsin B and β-actin in the normal and NPC1 fibroblasts treated with Baf A (400 nM), HP-β-CD (10 mM), and HEE-SS-PRX (1 mM β-CD) for 24 h. *D*, relative band intensity ratios of mature cathepsin B/pro-cathepsin B. The values are normalized with the untreated normal fibroblasts and expressed as the mean ± S.D. (*error bars*) ($n = 3$) (*, $p < 0.05$; *NS*, not significant).

6.0) (44). Compared with the untreated normal fibroblasts, the number of $mRFP^+$-GFP^+ yellow puncta (autophagosomes) increased, and the number of $mRFP^+$-GFP^- red puncta (autolysosomes) decreased remarkably in the untreated NPC1 fibroblasts. HP-β-CD treatment slightly increased the number of $mRFP^+$-GFP^+ yellow puncta, but a negligible change was observed in the number of $mRFP^+$-GFP^- red puncta compared with the untreated NPC1 fibroblasts. Note that HEE-SS-PRX treatment decreased the number of $mRFP^+$-GFP^+ yellow puncta and increased the number of $mRFP^+$-GFP^- red puncta in the NPC1 fibroblasts to levels comparable with those observed in the normal fibroblasts.

There are two possible reasons to explain the results of HP-β-CD and HEE-SS-PRX treatments in the mRFP-GFP-LC3 reporter experiments; these treatments (i) inhibited or promoted the fusion of autophagosomes and lysosomes or (ii) changed the lysosomal pH or lysosomal enzymatic activity. To discriminate between these two possibilities, the lysosomal enzymatic activity in the treated NPC1 fibroblasts was investigated by assessing the activity and the maturation of cathepsin B, one of the major lysosomal cysteine proteases (45, 46). The enzymatic activity and the maturation of cathepsin B were suppressed by Baf A treatment due to the neutralization of the acidic lysosomes (Fig. 6*A*–*D*) (47, 48). By contrast, both HP-β-CD and HEE-SS-PRX treatments caused negligible effects on the enzymatic activity and the maturation of cathepsin B in the NPC1 fibroblasts, indicating that the results of the mRFP-GFP-LC3 reporter experiments were attributable to the fusion of autophagosomes and lysosomes.

The Effects of HP-β-CD and Biocleavable Polyrotaxanes on the Colocalization of Autophagosomes and Lysosomes—To further confirm the facilitated maturation of autophagosomes in NPC1 fibroblasts by HEE-SS-PRX, the colocalization of the transiently expressed mRFP-LC3 with LAMP1-positive puncta was investigated (Fig. 7, *A* and *B*). Consistent with the mRFP-GFP-LC3 reporter experiments, the colocalization percentage of LAMP1 and mRFP-LC3 in the NPC1 fibroblasts was lower than in the normal fibroblasts, indicating that the mutation of NPC1 perturbed the maturation of autophagosomes. HP-β-CD treatment further decreased the colocalization percentage of mRFP-LC3 with LAMP1 in the NPC1 fibroblasts. HEE-SS-PRX treatment increased the colocalization percentage, indicating that the HEE-SS-PRX facilitated the formation of autolysosomes in the NPC1 fibroblasts. We also confirmed the colocalization of endogenous LC3 and LAMP1 in the treated NPC1 fibroblasts by immunostaining. Consistent with Fig. 7, most of the LC3-positive puncta were colocalized with LAMP1-positive puncta after the treatment with HEE-SS-PRX (data not

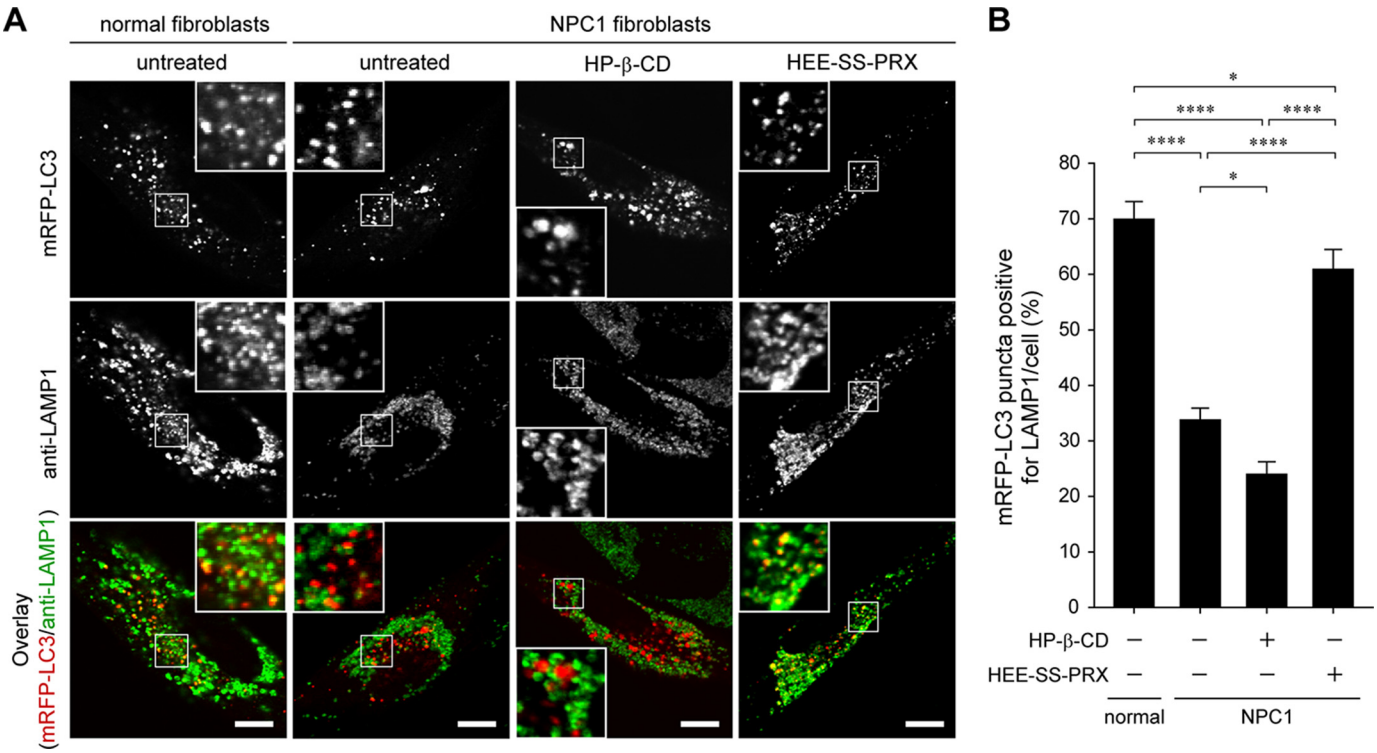

FIGURE 7. **Biocleavable polyrotaxanes facilitated the colocalization of LC3 and LAMP1.** *A*, CLSM images of mRFP-LC3 (*first row*) and anti-LAMP1 staining (*second row*) and overlay images (*third row*) in normal and NPC1 fibroblasts expressing mRFP-LC3 treated with HP-β-CD (10 mM) and HEE-SS-PRX (1 mM β-CD) for 24 h (*scale bars*, 20 μm). *B*, colocalization percentage of mRFP-LC3-positive puncta to anti-LAMP1-positive puncta. The values are expressed as the mean ± S.E. (*error bars*) of 30 cells (*, $p < 0.05$; ****, $p < 0.001$).

shown). These results further confirm that the HEE-SS-PRX facilitated the maturation of accumulated autophagosomes in NPC1 fibroblasts.

The Effects of α-CD-threaded Polyrotaxanes and Other β-CD Derivatives—To clarify the effects of the ring size of cyclodextrins on cholesterol reduction and autophagy response in NPC1 fibroblasts, two sets of α-CD-threaded PRXs composed of PEG/α-CD or Pluronic P123/α-CD were synthesized. Because the binding affinity of α-CD (six glucose units) to cholesterol is lower than for β-CD (seven glucose units) (49), the lysosomal cholesterols in NPC1 fibroblasts were only minimally reduced by treatment with the two sets of α-CD-threaded PRXs or α-CD alone (Fig. 8, *A* and *B*). Additionally, the levels of LC3-II and p62 in NPC1 fibroblasts remained unchanged by the two sets of α-CD-threaded PRXs or α-CD alone (Fig. 8*C*). These results suggest that the effect of biocleavable PRXs on facilitating the autophagic flux in NPC1 fibroblasts is related to the ability to reduce the lysosomal cholesterol level.

We also demonstrated the autophagy response of the NPC1 fibroblasts after the treatment with DM-β-CD, which has a higher binding affinity for cholesterols than does HP-β-CD (50). DM-β-CD showed a greater ability in reducing lysosomal cholesterols in the NPC1 fibroblasts (Fig. 8*D*) and induced a higher level of cholesterol extraction from the plasma membrane than did HP-β-CD (Fig. 8*E*). The levels of LC3-II and p62 in the NPC1 fibroblasts treated with DM-β-CD were higher than in those treated with HP-β-CD (Fig. 8*F*). According to these results, it is plausible that the effect of β-CD derivatives on the inhibition of autophagic flux is related to the cholesterol binding affinity of β-CD derivatives or the ability of cholesterol extraction from the plasma membrane.

DISCUSSION

Impaired autophagy in lysosomal storage disorder is of significant importance, not only for an understanding of the symptoms but also for finding a therapeutic method. In NPC disease, increased levels of LC3-positive puncta was observed even under basal conditions. This result can be attributed to various possibilities, such as the alteration of lysosomal enzymatic activities (32), the activation of Beclin-1 (30), and the impairment of autophagosome maturation (33). Our present results suggest that the perturbation of autophagosome-lysosome fusion is a major issue in NPC disease because negligible change in lysosomal enzymatic activities and Beclin-1 expression was observed in the human models of NPC1 fibroblasts (Figs. 3*A*, 5, and 7). It is clear that basal autophagic flux decreased in the NPC1 fibroblasts compared with the normal fibroblasts, but it is not completely inhibited because the levels of LC3-II and p62 in the untreated NPC1 fibroblasts are lower than in the Baf A-treated cells (Fig. 3).

There are various reports on the effects of HP-β-CD or β-CD derivatives on autophagy. Fujimoto and co-workers (51) have reported that methyl-β-CD increases the number of autophagosomes, presumably due to the extraction of cholesterols from the plasma membranes. Segatori and co-workers (52) have reported that HP-β-CD induces autophagy through the activation of transcription factor EB. Arima and co-workers (53) have reported that folate-appended methyl-β-CD induces

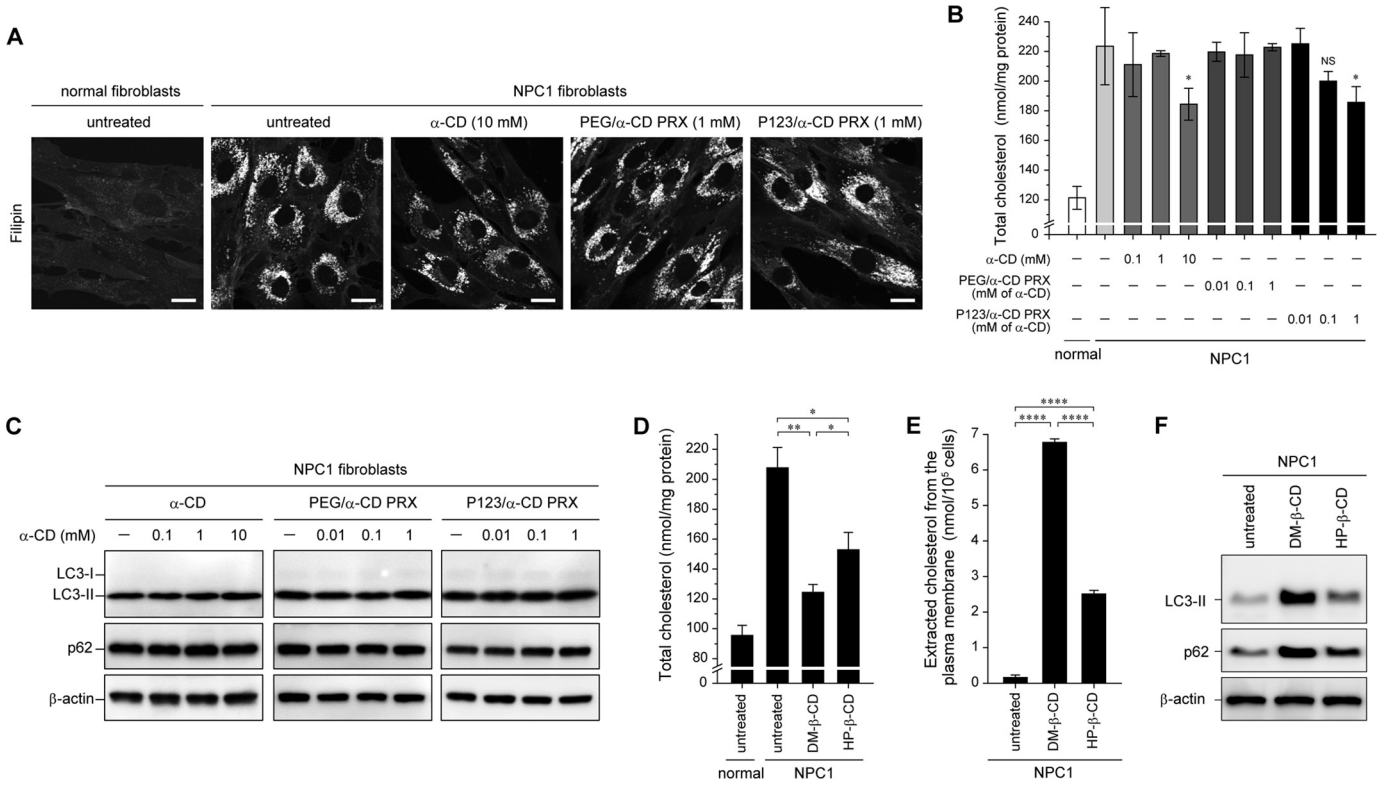

FIGURE 8. **The effect of α-CD-threaded PRXs and other β-CD derivatives on autophagic flux.** *A*, filipin staining for cholesterol in normal and NPC1 fibroblasts treated with α-CD (10 mM), PEG/α-CD PRX (1 mM α-CD), and P123/α-CD PRX (1 mM α-CD) for 24 h (*scale bars*, 20 μm). *B*, the amount of total cholesterol in normal and NPC1 fibroblasts treated with α-CD, PEG/α-CD PRX, and P123/α-CD PRX at various concentrations for 24 h ($n = 3$) (*, $p < 0.05$ against untreated NPC1 fibroblasts; *NS*, not significant). *C*, immunoblot analysis for LC3, p62, and β-actin in the NPC1 fibroblasts treated with α-CD, PEG/α-CD PRX, and P123/α-CD PRX at various concentrations for 24 h. *D*, the amount of total cholesterol in the normal and NPC1 fibroblasts treated with DM-β-CD (1 mM) and HP-β-CD (1 mM) for 24 h ($n = 3$) (*, $p < 0.05$; **, $p < 0.01$). *E*, the amount of cholesterol extracted from the plasma membrane to the culture medium after the treatment with DM-β-CD (10 mM) and HP-β-CD (10 mM) for 2 h at 4 °C ($n = 3$) (****, $p < 0.001$). *F*, immunoblot analysis for LC3, p62, and β-actin in the NPC1 fibroblasts treated with DM-β-CD (1 mM) and HP-β-CD (1 mM) for 24 h. The values are expressed as the mean ± S.D. (*error bars*).

autophagy in folate receptor-expressing cancer cells. Jaenisch and co-workers (33) have reported that treatment with a high concentration of HP-β-CD induces the cytoplasmic accumulation of autophagosomes and perturbs the protein degradation in *Npc1*$^{-/-}$ mouse embryonic fibroblasts. We confirmed that HP-β-CD treatment increased the levels of both LC3-II and p62 in a time-dependent manner in the NPC1 fibroblasts, consistent with the report of Jaenisch and co-workers (Figs. 2 and 3) (33). Also, our results indicate that HP-β-CD treatment only minimally induced dephosphorylation of p70S6k and 4E-BP1, indicating that the levels of LC3-II and p62 increased by HP-β-CD were not attributable to an mTOR-dependent autophagy (Fig. 3). Additionally, HP-β-CD did not decrease lysosomal enzymatic activity (Fig. 6). These results suggest that HP-β-CD perturbs autophagic flux without affecting mTORCa activity and lysosomal enzymatic activity.

Notably, the β-CD-threaded PRXs improved the impaired autophagic flux in NPC disease. The HEE-SS-PRX treatment showed negligible induction of mTOR-dependent autophagy, and a long incubation time was required to induce a decline in the levels of LC3-II and p62 (24 h) compared with the mTOR-dependent autophagy induced by the amino acid starvation (2 h) (Fig. 3). This suggests that for reducing LC3-II and p62 levels, the mechanism of action by which HEE-SS-PRX works is different from the starvation-induced autophagy. The mRFP-GFP-LC3 reporter experiments and the result of mRFP-LC3 and LAMP1 colocalization revealed that HEE-SS-PRX may promote the fusion of autophagosomes and lysosomes (Figs. 5 and 7). Because the HEE-SS-PRX also had no effect on the lysosomal enzymatic activity (Fig. 6) and the reduction of LC3-II and p62 was not observed in the presence of Baf A (Fig. 3*D*), it is reasonable to consider that the reduction of LC3-II and p62 levels by HEE-SS-PRX could be due to the promotion of autophagosome maturation.

Ballabio and co-workers (54) have reported that lysosomal cholesterol accumulation inhibits the fusion of endosomes-lysosomes and endosomes-autophagosomes in two model cells of lysosomal storage disorders. These authors have shown that the soluble *N*-ethylmaleimide-sensitive factor attachment protein (SNAP) receptors (SNAREs), such as VAMP7, Vti1b, and syntaxin 7, are preferentially sequestered to these cholesterol-enriched compartments. Enrich and co-workers (55) have reported the mislocalization of syntaxin 6 to endosomes instead of to the *trans*-Golgi network in NPC1-mutated Chinese hamster ovary cells. Accordingly, lysosomal cholesterol accumulation may cause the mislocalization of these transmembrane proteins to inhibit membrane fusion. Therefore, it is hypothesized that the localization of syntaxin 17 or VAMP8, essential factors in the fusion of autophagosomes with lysosomes (56, 57), might be altered by excess cholesterols, perturbing the fusion of autophagosomes with lysosomes. If this is true, then the reduction in lysosomal cholesterol by HEE-SS-PRX would

be expected to improve the localization of these fusion factors. When we demonstrated the autophagy response of α-CD-threaded PRXs, which induced lower lysosomal cholesterol reductions than the β-CD-threaded PRXs, negligible change in the levels of LC3-II and p62 was observed (Figs. 2 and 8, *A* and *B*). Although the detailed mechanism is still controversial, lysosomal cholesterol reduction by β-CD-threaded biocleavable HEE-SS-PRXs played a pivotal role in the improvement of autophagic flux in the NPC1 fibroblasts.

Nevertheless, it is not known why the treatment with β-CD did not improve the impaired autophagic flux in NPC1 fibroblasts, although it was able to reduce lysosomal cholesterols at a high concentration (10 mM). Note that HP-β-CD increased the levels of LC3-II and p62, even in the normal fibroblasts (Fig. 3*C*). Additionally, DM-β-CD induced higher levels of LC3-II and p62 than did HP-β-CD (Fig. 8, *D* and *E*). The critical difference between HP-β-CD and HEE-SS-PRX is the ability to extract cholesterols at the plasma membrane (Fig. 2*C*). Because the hydrophobic cavity of β-CD is occupied with the polymer chain in the PRX structure, this unique structure does not permit the further inclusion of other molecules into the cavity of β-CD. In reality, HEE-SS-PRX has shown negligible interaction with the plasma membrane and becomes internalized into cells via endocytosis (12). By contrast, HP-β-CD interacts with the plasma membrane to extract cholesterols due to the exposure of its hydrophobic cavity (Fig. 2*C*). It is known that the cholesterol extraction from the plasma membrane via β-CD perturbs the formation of clathrin pit budding, leading to an inhibition of endocytosis (58, 59). It is reported that the clathrin is a key factor in autophagy-related events, such as autophagic lysosome reformation (60). It is hypothesized that the extraction of cholesterols from the plasma membrane via HP-β-CD affects the process of autophagic flux.

In this study, we have shown that HEE-SS-PRX can simultaneously improve lysosomal cholesterol accumulation and autophagy impairment in NPC disease. To date, no drugs have been reported that can improve both lysosomal cholesterol accumulation and autophagy impairment in NPC disease. For example, rapamycin is reported to improve autophagy impairment in NPC disease but has negligible effects on lysosomal cholesterols (33). *N*-Butyldeoxynojirimycin improves the clinical symptoms of NPC disease (61) but has a negligible effect on autophagy in NPC disease model cells (30). Therefore, our designed β-CD-threaded biocleavable PRXs have great potential for the treatment of NPC disease. However, it is important to note that delivery of the therapeutics to the brain is required for ameliorating the neurodegeneration in NPC disease. The body disposition and the delivery efficacy of biocleavable PRXs to the brain are currently being investigated in our laboratory as well as the molecular design of PRXs to cross the blood brain barrier.

Acknowledgments—We deeply appreciate Prof. Noboru Mizushima (Tokyo University) for helpful discussions and critical reading of the paper. We acknowledge Prof. Tamotsu Yoshimori (Osaka University) for providing pmRFP-GFP-LC3 and pmRFP-LC3.

REFERENCES

1. Futerman, A. H., and van Meer, G. (2004) The cell biology of lysosomal storage disorders. *Nat. Rev. Mol. Cell Biol.* **5,** 554–565
2. Platt, F. M., Boland, B., and van der Spoel, A. C. (2012) The cell biology of disease: lysosomal storage disorders: the cellular impact of lysosomal dysfunction. *J. Cell Biol.* **199,** 723–734
3. Carstea, E. D., Morris, J. A., Coleman, K. G., Loftus, S. K., Zhang, D., Cummings, C., Gu, J., Rosenfeld, M. A., Pavan, W. J., Krizman, D. B., Nagle, J., Polymeropoulos, M. H., Sturley, S. L., Ioannou, Y. A., Higgins, M. E., Comly, M., Cooney, A., Brown, A., Kaneski, C. R., Blanchette-Mackie, E. J., Dwyer, N. K., Neufeld, E. B., Chang, T. Y., Liscum, L., Strauss, J. F., 3rd, Ohno, K., Zeigler, M., Carmi, R., Sokol, J., Markie, D., O'Neill, R. R., van Diggelen, O. P., Elleder, M., Patterson, M. C., Brady, R. O., Vanier, M. T., Pentchev, P. G., and Tagle, D. A. (1997) Niemann-Pick C1 disease gene: homology to mediators of cholesterol homeostasis. *Science* **277,** 228–231
4. Vanier, M. T., and Millat, G. (2003) Niemann-Pick disease type C. *Clin. Genet.* **64,** 269–281
5. Chang, T. Y., Reid, P. C., Sugii, S., Ohgami, N., Cruz, J. C., Chang, C. C. Y. (2005) Niemann-Pick type C disease and intracellular cholesterol trafficking. *J. Biol. Chem.* **280,** 20917–20920
6. Liu, B., Turley, S. D., Burns, D. K., Miller, A. M., Repa, J. J., and Dietschy, J. M. (2009) Reversal of defective lysosomal transport in NPC disease ameliorates liver dysfunction and neurodegeneration in the *npc1*$^{-/-}$ mouse. *Proc. Natl. Acad. Sci. U.S.A.* **106,** 2377–2382
7. Davidson, C. D., Ali, N. F., Micsenyi, M. C., Stephney, G., Renault, S., Dobrenis, K., Ory, D. S., Vanier, M. T., and Walkley, S. U. (2009) Chronic cyclodextrin treatment of murine Niemann-Pick C disease ameliorates neuronal cholesterol and glycosphingolipid storage and disease progression. *PLoS One* **4,** e6951
8. Porter, F. D., Scherrer, D. E., Lanier, M. H., Langmade, S. J., Molugu, V., Gale, S. E., Olzeski, D., Sidhu, R., Dietzen, D. J., Fu, R., Wassif, C. A., Yanjanin, N. M., Marso, S. P., House, J., Vite, C., Schaffer, J. E., and Ory, D. S. (2010) Cholesterol oxidation products are sensitive and specific blood-based biomarkers for Niemann-Pick C1 disease. *Sci. Transl. Med.* **2,** 56ra81
9. Matsuo, M., Togawa, M., Hirabaru, K., Mochinaga, S., Narita, A., Adachi, M., Egashira, M., Irie, T., and Ohno, K. (2013) Effects of cyclodextrin in two patients with Niemann-Pick type C disease. *Mol. Genet. Metab.* **108,** 76–81
10. Harada, A., Hashidzume, A., Yamaguchi, H., and Takashima, Y. (2009) Polymeric Rotaxanes. *Chem. Rev.* **109,** 5974–6023
11. Tamura, A., and Yui, N. (2014) Threaded macromolecules as a versatile framework for biomaterials. *Chem. Commun.* **50,** 13433–13446
12. Tamura, A., and Yui, N. (2014) Lysosomal-specific cholesterol reduction by biocleavable polyrotaxanes for ameliorating Niemann-Pick type C disease. *Sci. Rep.* **4,** 4356
13. Mizushima, N., Levine, B., Cuervo, A. M., and Klionsky, D. J. (2008) Autophagy fights disease through cellular self-digestion. *Nature* **451,** 1069–1075
14. Shintani, T., and Klionsky, D. J. (2004) Autophagy in health and disease: a double-edged sword. *Science* **306,** 990–995
15. Levine, B., and Kroemer, G. (2008) Autophagy in the pathogenesis of disease. *Cell* **132,** 27–42
16. Jiang, P., and Mizushima, N. (2014) Autophagy and human diseases. *Cell Res.* **24,** 69–79
17. Hara, T., Nakamura, K., Matsui, M., Yamamoto, A., Nakahara, Y., Suzuki-Migishima, R., Yokoyama, M., Mishima, K., Saito, I., Okano, H., and Mizushima, N. (2006) Suppression of basal autophagy in neural cells causes neurodegenerative disease in mice. *Nature* **441,** 885–889
18. Komatsu, M., Waguri, S., Chiba, T., Murata, S., Iwata, J., Tanida, I., Ueno, T., Koike, M., Uchiyama, Y., Kominami, E., and Tanaka, K. (2006) Loss of autophagy in the central nervous system causes neurodegeneration in mice. *Nature* **441,** 880–884
19. Nixon, R. A. (2013) The role of autophagy in neurodegenerative disease. *Nat. Med.* **19,** 983–997
20. Lieberman, A. P., Puertollano, R., Raben, N., Slaugenhaupt, S., Walkley,

S. U., Ballabio, A. (2012) Autophagy in lysosomal storage disorders. *Autophagy* **8,** 719–730
21. Gabandé-Rodríguez, E., Boya, P., Labrador, V., Dotti, C. G., and Ledesma, M. D. (2014) High sphingomyelin levels induce lysosomal damage and autophagy dysfunction in Niemann Pick disease type A. *Cell Death Differ.* **21,** 864–875
22. Chévrier, M., Brakch, N., Céline, L., Genty, D., Ramdani, Y., Moll, S., Djavaheri-Mergny, M., Brasse-Lagnel, C., Annie Laquerrière, A. L., Barbey, F., and Bekri, S. (2010) Autophagosome maturation is impaired in Fabry disease. *Autophagy* **6,** 589–599
23. Takamura, A., Higaki, K., Kajimaki, K., Otsuka, S., Ninomiya, H., Matsuda, J., Ohno, K., Suzuki, Y., and Nanba, E. (2008) Enhanced autophagy and mitochondrial aberrations in murine G_{M1}-gangliosidosis. *Biochem. Biophys. Res. Commun.* **367,** 616–622
24. Settembre, C., Fraldi, A., Jahreiss, L., Spampanato, C., Venturi, C., Medina, D., de Pablo, R., Tacchetti, C., Rubinsztein, D. C., and Ballabio, A. (2008) A block of autophagy in lysosomal storage disorders. *Hum. Mol. Genet.* **17,** 119–129
25. Tanaka, Y., Guhde, G., Suter, A., Eskelinen, E. L., Hartmann, D., Lüllmann-Rauch, R., Janssen, P. M., Blanz, J., von Figura, K., and Saftig, P. (2000) Accumulation of autophagic vacuoles and cardiomyopathy in LAMP-2-deficient mice. *Nature* **406,** 902–906
26. Koike, M., Shibata, M., Waguri, S., Yoshimura, K., Tanida, I., Kominami, E., Gotow, T., Peters, C., von Figura, K., Mizushima, N., Saftig, P., and Uchiyama, Y. (2005) Participation of autophagy in storage of lysosomes in neurons from mouse models of neuronal ceroid-lipofuscinoses (Batten disease). *Am. J. Pathol.* **167,** 1713–1728
27. Liao, G., Yao, Y., Liu, J., Yu, Z., Cheung, S., Xie, A., Liang, X., and Bi, X. (2007) Cholesterol accumulation is associated with lysosomal dysfunction and autophagic stress in $Npc1^{-/-}$ mouse brain. *Am. J. Pathol.* **171,** 962–975
28. Ishibashi, S., Yamazaki, T., and Okamoto, K. (2009) Association of autophagy with cholesterol-accumulated compartments in Niemann-Pick disease type C cells. *J. Clin. Neurosci.* **16,** 954–959
29. Ko, D. C., Milenkovic, L., Beier, S. M., Manuel, H., Buchanan, J., and Scott, M. P. (2005) Cell-autonomous death of cerebellar purkinje neurons with autophagy in Niemann-Pick type C disease. *PLoS Genet.* **1,** 81–95
30. Pacheco, C. D., Kunkel, R., and Lieberman, A. P. (2007) Autophagy in Niemann-Pick C disease is dependent upon Beclin-1 and responsive to lipid trafficking defects. *Hum. Mol. Genet.* **16,** 1495–1503
31. Ordonez, M. P., Roberts, E. A., Kidwell, C. U., Yuan, S. H., Plaisted, W. C., and Goldstein, L. S. (2012) Disruption and therapeutic rescue of autophagy in a human neuronal model of Niemann Pick type C1. *Hum. Mol. Genet.* **21,** 2651–2662
32. Elrick, M. J., Yu, T., Chung, C., and Lieberman, A. P. (2012) Impaired proteolysis underlies autophagic dysfunction in Niemann-Pick type C disease. *Hum. Mol. Genet.* **21,** 4876–4887
33. Sarkar, S., Carroll, B., Buganim, Y., Maetzel, D., Ng, A. H., Cassady, J. P., Cohen, M. A., Chakraborty, S., Wang, H., Spooner, E., Ploegh, H., Gsponer, J., Korolchuk, V. I., and Jaenisch, R. (2013) Impaired autophagy in the lipid-storage disorder Niemann-Pick type C1 disease. *Cell Rep.* **5,** 1302–1315
34. Tamura, A., and Yui, N. (2013) Cellular internalization and gene silencing of siRNA polyplexes by cytocleavable cationic polyrotaxanes with tailored rigid backbones. *Biomaterials* **34,** 2480–2491
35. Kimura, S., Noda, T., and Yoshimori, T. (2007) Dissection of the autophagosome maturation process by a novel reporter protein, tandem fluorescent-tagged LC3. *Autophagy* **3,** 452–460
36. Kabeya, Y., Mizushima, N., Ueno, T., Yamamoto, A., Kirisako, T., Noda, T., Kominami, E., Ohsumi, Y., and Yoshimori, T. (2000) LC3, a mammalian homologue of yeast Apg8p, is localized in autophagosome membranes after processing. *EMBO J.* **19,** 5720–5728
37. Kabeya, Y., Mizushima, N., Yamamoto, A., Oshitani-Okamoto, S., Ohsumi, Y., and Yoshimori, T. (2004) LC3, GABARAP and GATE16 localize to autophagosomal membrane depending on form-II formation. *J. Cell Sci.* **117,** 2805–2812
38. Bjørkøy, G., Lamark, T., Brech, A., Outzen, H., Perander, M., Overvatn, A., Stenmark, H., and Johansen, T. (2005) p62/SQSTM1 forms protein aggregates degraded by autophagy and has a protective effect on huntingtin-induced cell death. *J. Cell Biol.* **171,** 603–614
39. Klionsky, D. J., Elazar, Z., Seglen, P. O., and Rubinsztein, D. C. (2008) Does bafilomycin A1 block the fusion of autophagosomes with lysosomes? *Autophagy* **4,** 849–850
40. Sengupta, S., Peterson, T. R., and Sabatini, D. M. (2010) Regulation of the mTOR complex 1 pathway by nutrients, growth factors, and stress. *Mol. Cell.* **40,** 310–322
41. Noda, T., and Ohsumi, Y. (1998) Tor, a phosphatidylinositol kinase homologue, controls autophagy in yeast. *J. Biol. Chem.* **273,** 3963–3966
42. Laplante, M., and Sabatini, D. M. (2012) mTOR signaling in growth control and disease. *Cell* **149,** 274–293
43. Gingras, A. C., Kennedy, S. G., O'Leary, M. A., Sonenberg, N., and Hay, N. (1998) 4E-BP1, a repressor of mRNA translation, is phosphorylated and inactivated by the Akt(PKB) signaling pathway. *Genes Dev.* **12,** 502–513
44. Shaner, N. C., Steinbach, P. A., and Tsien, R. Y. (2005) A guide to choosing fluorescent proteins. *Nat. Methods* **2,** 905–909
45. Chapman, H. A., Riese, R. J., and Shi, G. P. (1997) Emerging roles for cysteine proteases in human biology. *Annu. Rev. Physiol.* **59,** 63–88
46. Ni, H. M., Bockus, A., Wozniak, A. L., Jones, K., Weinman, S., Yin, X. M., and Ding, W. X. (2011) Dissecting the dynamic turnover of GFP-LC3 in the autolysosome. *Autophagy* **7,** 188–204
47. Mach, L., Mort, J. S., and Glössl, J. (1994) Maturation of human procathepsin B. *J. Biol. Chem.* **269,** 13030–13035
48. Punturieri, A., Filippov, S., Allen, E., Caras, I., Murray, R., Reddy, V., and Weiss, S. J. (2000) Regulation of elastinolytic cysteine proteinase activity in normal and cathepsin K-deficient human macrophages. *J. Exp. Med.* **192,** 789–799
49. Motoyama, K., Arima, H., Toyodome, H., Irie, T., Hirayama, F., and Uekama, K. (2006) Effect of 2,6-di-*O*-methyl-α-cyclodextrin on hemolysis and morphological change in rabbit's red blood cells. *Eur. J. Pharm. Sci.* **29,** 111–119
50. Motoyama, K., Kameyama, K., Onodera, R., Araki, N., Hirayama, F., Uekama, K., and Arima, H. (2009) Involvement of PI3K-Akt-Bad pathway in apoptosis induced by 2,6-di-O-methyl-β-cyclodextrin, not 2,6-di-O-methyl-α-cyclodextrin, through cholesterol depletion from lipid rafts on plasma membranes in cells. *Eur. J. Pharm. Sci.* **38,** 249–261
51. Cheng, J., Ohsaki, Y., Tauchi-Sato, K., Fujita, A., and Fujimoto, T. (2006) Cholesterol depletion induces autophagy. *Biochem. Biophys. Res. Commun.* **351,** 246–252
52. Song, W., Wang, F., Lotfi, P., Sardiello, M., and Segatori, L. (2014) 2-Hydroxypropyl-β-cyclodextrin promotes transcription factor EB-mediated activation of autophagy: implications for therapy. *J. Biol. Chem.* **289,** 10211–10222
53. Onodera, R., Motoyama, K., Tanaka, N., Ohyama, A., Okamatsu, A., Higashi, T., Kariya, R., Okada, S., and Arima, H. (2014) Involvement of autophagy in antitumor activity of folate-appended methyl-β-cyclodextrin. *Sci. Rep.* **4,** 4417
54. Fraldi, A., Annunziata, F., Lombardi, A., Kaiser, H. J., Medina, D. L., Spampanato, C., Fedele, A. O., Polishchuk, R., Sorrentino, N. C., Simons, K., and Ballabio, A. (2010) Lysosomal fusion and SNARE function are impaired by cholesterol accumulation in lysosomal storage disorders. *EMBO J.* **29,** 3607–3620
55. Reverter, M., Rentero, C., Garcia-Melero, A., Hoque, M., Vilà de Muga, S., Alvarez-Guaita, A., Conway, J. R., Wood, P., Cairns, R., Lykopoulou, L., Grinberg, D., Vilageliu, L., Bosch, M., Heeren, J., Blasi, J., Timpson, P., Pol, A., Tebar, F., Murray, R. Z., Grewal, T., and Enrich, C. (2014) Cholesterol regulates Syntaxin 6 trafficking at trans-Golgi network endosomal boundaries. *Cell Rep.* **7,** 883–897
56. Itakura, E., Kishi-Itakura, C., and Mizushima, N. (2012) The hairpin-type tail-anchored SNARE syntaxin 17 targets to autophagosomes for fusion with endosomes/lysosomes. *Cell* **151,** 1256–1269
57. Furuta, N., Fujita, N., Noda, T., Yoshimori, T., and Amano, A. (2010) Combinational soluble *N*-ethylmaleimide-sensitive factor attachment protein receptor proteins VAMP8 and Vti1b mediate fusion of antimicrobial and canonical autophagosomes with lysosomes. *Mol. Biol. Cell* **21,** 1001–1010
58. Subtil, A., Gaidarov, I., Kobylarz, K., Lampson, M. A., Keen, J. H., and

McGraw, T. E. (1999) Acute cholesterol depletion inhibits clathrin-coated pit budding. *Proc. Natl. Acad. Sci. U.S.A.* **96,** 6775–6780
59. Rodal, S. K., Skretting, G., Garred, O., Vilhardt, F., van Deurs, B., and Sandvig, K. (1999) Extraction of cholesterol with methyl-β-cyclodextrin perturbs formation of clathrin-coated endocytic vesicles. *Mol. Biol. Cell* **10,** 961–974
60. Rong, Y., Liu, M., Ma, L., Du, W., Zhang, H., Tian, Y., Cao, Z., Li, Y., Ren, H., Zhang, C., Li, L., Chen, S., Xi, J., and Yu, L. (2012) Clathrin and phosphatidylinositol-4,5-bisphosphate regulate autophagic lysosome reformation. *Nat. Cell Biol.* **14,** 924–934
61. Patterson, M. C., Vecchio, D., Prady, H., Abel, L., and Wraith, J. E. (2007) Miglustat for treatment of Niemann-Pick C disease: a randomised controlled study. *Lancet Neurol.* **6,** 765–772